Journal of the Serbian Chemical Society
JSCS-info@shd.org.rs • www.shd.org.rs/JSCS
J. Serb. Chem. Soc. 90 (9) 1119–1130 (2025)
JSCS–5443
Original scientific paper
Published 30 September, 2025

Ni–Bi–Sn ternary system liquidus surface projection

CHINGIZ I. ABILOV[1]*, IKHTIYAR B. BAKHTIYARLY[2], SAYYARA H. SADIGOVA[1], MEHRIBAN SH. HASANOVA[1] and ELMIRA K. GASIMOVA[1]

[1]*Azerbaijan Technical University, Baku, Azerbaijan and* [2]*Institute of Catalysis and Inorganic Chemistry named after academician M. Naghiyev of the Ministry of Science and Education of the Republic of Azerbaijan*

(Received 5 March, revised 8 May, accepted 15 June 2025)

Abstract: Physicochemical analysis investigations were conducted on six internal polythermic sections of the Ni–Bi–Sn ternary system, and phase diagrams of the sections were constructed. It was determined that two of the sections were quasibinary, and four were non-quasibinary. The projection of the liquidus surface of the ternary system was constructed. The equations for the nonvariant equilibrium reactions occurring in the ternary system were compiled and their coordinates were determined. The presence of promising solid solution areas was revealed in some of the internal sections of the ternary system, and their boundaries at room temperature were determined. The absence of new complex compounds and the presence of homogeneous regions indicate that the synthesized materials could be suitable for application as switching and contact layers in alternative energy sources.

Keywords: phase diagrams; alloys; primary crystallization; nonvariant reactions.

INTRODUCTION

Metallic nickel and its alloys are widely used in metallurgy as doping elements to enhance the mechanical properties of steel and increase resistance to heat and corrosion. They are also employed in the production of military ammunition, and in electronics and electrical engineering for materials like invar, platinite and nichrome. Nickel and its alloys also exhibit catalytic properties. Considering that nickel alloys find applications as both active (working element of the thermoelectric device) and passive (commutation layers) materials in thermoelectric energy converters,[1–5] the need to study the synthesis and properties of nickel-based alloys is clear.

Bi–Sn alloys are widely employed as contact materials in solid-state electronic devices and equipment. However, their low melting temperatures (both of the con-

* Corresponding author. E-mail: chingiz.ebilov@aztu.edu.az
https://doi.org/10.2298/JSC250305045A

stituent elements and the alloys themselves) can lead to heating when current passes through the contacts, potentially resulting in contact failure. Including a substance with a high melting point and good mechanical resistance, such as nickel, into these materials could offer a solution. Furthermore, the chemical compatibility of the interacting substances plays a crucial role. It is essential to consider the potential formation of new phases resulting from interactions between the contacting substances, the reactions that occur, and their formation temperatures, as these new phases can cause contact failure or reduce conductivity. Therefore, a thorough physicochemical analysis of the Ni–Bi–Sn system is of significant technological relevance.

Results of some studies on the Ni–Bi–Sn system have been reported in the literature. For example, Vassilev *et al*.[6] studied the solid phase equilibria of the ternary system at 733 and 903 K and scanning electron microscopy results indicated the presence of a ternary compound with the formula Ni_7Sn_2Bi. However, X-ray diffraction analysis did not confirm this compound. Thus, despite the modernity of these two investigation methods, inconsistencies exist in their reported results.

Thermodynamic functions of some ternary phases were calculated using parameters from the binary systems of the Ni–Bi–Sn triangle, and the system's phase equilibrium was subsequently studied based on these results.[7,8] Naturally, thermodynamic calculations alone cannot provide complete clarity on the ternary system's phase equilibrium. Furthermore, the activity coefficient of bismuth in the liquid phase at 1773 K was obtained using the isopiestic method, and these values were compared with theoretical calculations.[8]

The alloys of the Ni–Bi–Sn system were studied by X-ray diffraction analysis which indicated the presence of ternary compounds with the approximate formulas Ni_6Sn_2Bi and Ni_7Sn_2Bi.[9] According to the authors, the diffraction bands in the X-ray diffraction patterns of these ternary compounds coincide with the analogous diffraction maxima of NiBi and Ni_3Bi binary compounds. Consequently, the authors' conclusions are questionable, as assuming the existence of a new ternary compound based solely on X-ray phase analysis is methodologically unsound.

The Ni–Bi–Sn system was studied by SEM and differential scanning calorimetry, which showed that ternary eutectic reactions in the system occur at 116––129 °C.[10]

Thus, this brief literature review indicates that the Ni–Bi–Sn ternary system has not been fully studied and that existing studies present conflicting results. Therefore, a comprehensive study of the Ni–Bi–Sn system over a wide concentration and temperature range was deemed necessary, the results of which are presented herein. This study focuses significantly on investigating new sections, in addition to those traditionally examined in the literature.

EXPERIMENTAL

Ternary alloys were synthesized from special purity bismuth and tin (99.999 %), and TU-6-09 carbonyl grade nickel, using a single-temperature furnace with a vibratory mixer.[11,12] Depending on the composition, the synthesis temperature ranged from 1373 to 1573 K. To ensure equilibrium and complete reaction, the alloys were thermally treated (annealed) at temperatures of 363–523 K (composition-dependent) for 480 h. The alloys were obtained as dense masses with a dark-gray metallic colour. To clarify the nature of the chemical interaction between the components of the ternary system, differential thermal analysis (DTA), microstructural analysis (MSA) and X-ray phase analysis (XRD) were performed, and their microhardness and density were measured.

DTA was performed in the dynamic mode in an inert (helium) atmosphere with an STA 449F3 Jupiter simultaneous thermal analyzer (Netzsch, Germany) at a heating rate of 15 K/min using a Pt–Pt/Rh thermocouple. The analyzer operates under the control of the Proteus software. XRD analysis was performed on system samples with a D2 Phaser X-ray powder diffractometer (Bruker, Germany) using CuKα radiation and a Ni filter. The scanning speed was 2°/min. Device control and data analysis were managed using the Diffrac.Suite software package.[13,14]

MSA and microhardness measurements were performed on ground and polished samples using a “View” and “Micrometer-5101” microscopes, as well as on “PMT-3” microhardness tester with automatic load. The surfaces were etched with diluted nitric acid (2:1). Density was determined pycnometrically using toluene as the displacement liquid.

RESULTS AND DISCUSSION

The nature of chemical interactions in the Bi–Ni–Sn ternary system was investigated along the quasibinary sections Ni_3Sn–Bi and Ni_3Sn_2–Bi, and the non-quasibinary sections $Bi_{0.75}Sn_{0.25}$–$Ni_{0.5}Sn_{0.5}$, BiNi–Sn, $Bi_{0.6}Ni_{0.4}$–Sn and $Bi_{0.57}Sn_{0.43}$–Ni. The phase equilibria observed in these sections are described below.

Ni_3Sn–Bi Section

The Ni_3Sn–Bi phase diagram was constructed based on the results of physicochemical analysis. The section is quasibinary, and its phase diagram is of a simple eutectic type. However, its eutectic is degenerate. The eutectic occurs at ~270 °C. The phase transition in the Ni_3Sn compound, which occurs at 920 °C, is also identified in this phase diagram. However, due to the influence of bismuth, the temperature of this transition decreases to ~905 °C. A homogeneous region based on Ni_3Sn was observed in the section, and its boundary at room temperature corresponds to 1.5 mol % Bi. Given that nickel-containing alloys are recognized as effective materials for thermoelectric energy sources, the $(Ni_3Sn)_{1-x}Bi_x$ solid solutions identified in this section also hold significant promise for such applications.

Ni_3Sn_2–Bi Section

The phase diagram of this section also exhibits a simple eutectic type, indicating it is a quasi-binary system. The eutectic occurs at approximately 267 °C and

~99 mol % Bi. The phase diagram indicates no solid solution formation based on Ni_3Sn_2. As eutectic compositions inherently form composite materials and are utilized in switching and contact networks, the eutectic compositions identified in this section are promising for solid-state electronic applications.

To determine the coordinates of nonvariant points, monovariant curves, isotherms, and primary crystallization fields in the projection of the Ni–Bi–Sn ternary system, a series of non-quasibinary sections were investigated. Let us elaborate on some of these sections which sufficiently reflect the nature of chemical interactions in the ternary system.

$Bi_{0.75}Sn_{0.25}$–$Ni_{0.5}Sn_{0.5}$ Section

The initial components of this section ($Bi_{0.75}Sn_{0.25}$–$Ni_{0.5}Sn_{0.5}$ and $Ni_{0.5}Sn_{0.5}$) are analogous to mechanical mixtures in their respective Bi–Sn and Ni–Sn binary systems. Using the aforementioned physicochemical analysis methods, the phase diagram for the $Bi_{0.75}Sn_{0.25}$–$Ni_{0.5}Sn_{0.5}$ section was constructed (Fig. 1).

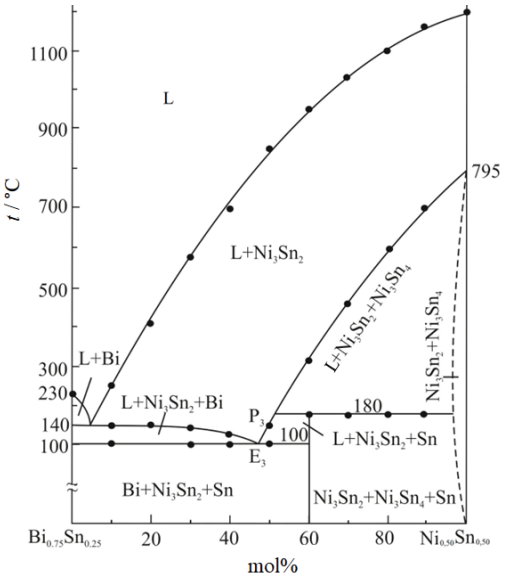

Fig. 1. Phase diagram of the $Bi_{0.75}Sn_{0.25}$–$Ni_{0.5}Sn_{0.5}$ section.

It is evident from the figure that the $Bi_{0.75}Sn_{0.25}$–$Ni_{0.5}Sn_{0.5}$ section is non-quasibinary and passes exclusively through the Bi–Ni_3Sn_2–Sn subsystem region, crossing two crystallization fields of Bi and Ni_3Sn_2. Consequently, its liquidus comprises two branches corresponding to the primary crystallization of Bi and Ni_3Sn_2.

These branches intersect where the section crosses the monovariant curve at 130 °C. At this point, binary crystallization (L+Ni_3Sn_2+Bi) begins and proceeds along the monovariant curve until it reaches the four-phase ternary eutectic point

(L ↔ Bi+Ni_3Sn+Sn) at 100 °C (48 mol % $Ni_{0.5}Sn_{0.5}$). In the sub-solidus region, within the concentration range of 0–60 mol % $Ni_{0.5}Sn_{0.5}$, a mixture of three phases (Bi+Ni_3Sn_2+Sn) precipitates. In the region rich in $Ni_{0.5}Sn_{0.5}$, the peritectic reaction L + Ni_3Sn_2 ↔ Ni_3Sn_4 starts at 795 °C (p_3), leading to the formation of the Ni_3Sn_4 compound. This reaction culminates in a four-phase ternary nonvariant peritectic equilibrium P_3 (L + Ni_3Sn_2 ↔ Ni_3Sn_4 + Sn) at 180 °C. Consequently, within the concentration range of 60–100 mol % $Ni_{0.5}Sn_{0.5}$, a mixture of Ni_3Sn_2 + Ni_3Sn_4 + Sn phases crystallizes. Practically no solubility was observed for either component.

The $Ni_{0.5}Sn_{0.5}$–Sn section is non-quasibinary. According to singular triangulation, it passes through the regions of three sub-systems formed by the quasibinary sections Bi–Ni_3Sn and Bi–Ni_3Sn_2: (Bi–Ni–Ni_3Sn (I), Bi–Ni_3Sn–Ni_3Sn_2 (II) and Bi–Ni_3Sn_2–Sn (III)), Fig. 2.

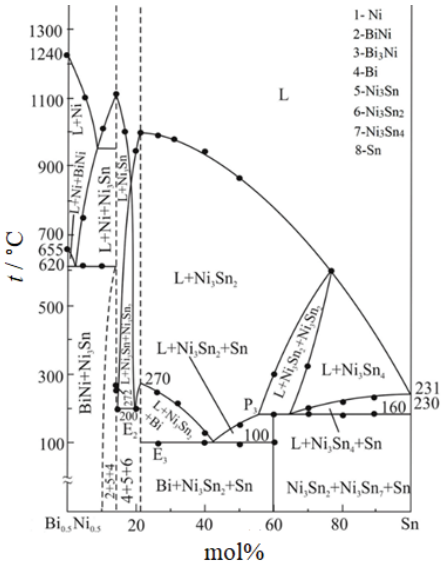

Fig. 2. Phase diagram of the $Bi_{0.5}Ni_{0.5}$–Sn section.

Therefore, the phase diagram of the $Bi_{0.5}Ni_{0.5}$–Sn section is divided into three parts. The first part (I) covers the concentration range of 0–14 mol % Sn. Here, the liquidus curve consists of two branches that intersect at the point where the section crosses the monovariant curve. These branches correspond to the primary crystallization of Ni and the Ni_3Sn compound.

The first component is within the composition of the BiNi compound, which is formed in the Bi—Ni binary system at 654 °C by the peritectic reaction L + Ni ↔ BiNi and melts incongruently. Here, the formation temperature of this compound begins to decrease. Finally, at 620 °C, both phases (L+Ni) that form the BiNi compound are in stoichiometric composition, so both are consumed simul-

taneously, and the process does not reach the four-phase ternary peritectic. As a result, two phases (BiNi+Ni_3Sn) precipitate in the subsolidus region.

The second part (II) of the $Bi_{0.5}Ni_{0.5}$–Sn section's phase diagram covers the concentration range of 14–22 mol % Sn. Here, the nature of the chemical interaction is relatively simple. The liquidus consists of two branches that characterize the primary crystallization of Ni_3Sn and Ni_3Sn_2, intersecting at the point where the section crosses the next monovariant curve. Crystallization ends at 200 °C with the four-phase ternary eutectic equilibrium L ↔ Bi + Ni_3Sn + Ni_3Sn_2.

In the subsolidus, a mixture of Bi+Ni_3Sn+Ni_3Sn_2 phases precipitates. In the third part (III), which falls within the Bi–Ni_3Sn_2–Sn quasi-ternary region (22–100 mol % Sn), the chemical interaction is somewhat more complex. Here, the $Bi_{0.5}Ni_{0.5}$–Sn section intersects two primary crystallization fields (Ni_3Sn_2 and Ni_3Sn_4), so it consists of two branches. The branches intersect at the point (76 mol % Sn) where the section crosses the monovariant curve that borders these primary crystallization fields, and binary crystallization (L+Ni_3Sn_2+Ni_3Sn_4) begins at that point.

In the phase diagram, within the concentration range of 22–60 mol % Sn, crystallization in the subsolidus ends with the four-phase ternary eutectic (E_3) reaction (L ↔ Bi + Ni_3Sn_2 + Sn) at 100 °C. Within the 60–100 mol % Sn concentration range, it ends with the four-phase ternary peritectic (P_3) equilibrium (L + Bi + Ni_3Sn_2 ↔ Ni_3Sn_4 + Sn) at 180 °C.

$Bi_{0.6}Ni_{0.4}$–Sn Section

This section is parallel to the $Bi_{0.5}Ni_{0.5}$–Sn section (Fig. 2) and passes through a relatively close concentration plane. In other words, the $Bi_{0.6}Ni_{0.4}$–Sn section also passes through the regions of three subsystems: Bi–Ni–Ni_3Sn (I), Bi–Ni_3Sn––Ni_3Sn_2 (II) and Bi–Ni_3Sn_2–Sn (III). Its phase diagram (Fig. 3) is non-quasibinary and is divided into three parts. With the exception of the first part (I), the nature of the chemical interaction in the second (II) and third (III) parts is almost identical.

In the first part (I), the liquidus consists of two branches because the section intersects the monovariant curve at the boundary of the primary crystallization fields of the Ni and Ni_3Sn phases (6 mol % Sn). Crystallization passes through the nonvariant peritectic equilibria P_1 (L + Ni ↔ BiNi + Ni_3Sn, 600 °C) and P_2 (L + BiNi ↔ Bi_3Ni + Ni_3Sn, 430 °C) and ends at the four-phase ternary eutectic equilibrium E_1 (L ↔ Bi + Bi_3Ni + Ni_3Sn, 250 °C). In the subsolidus, Bi+Bi_3Ni+Ni_3Sn phases crystallize together.

In the second (II) and third (III) parts of the phase diagram, the shape of the liquidus curve is similar to that in the $Bi_{0.5}Ni_{0.5}$–Sn section. However, crystallization ends with the nonvariant eutectic equilibria E_2 (II – 12–18 mol % Sn), E_3 (III – 18–66 mol % Sn), and the nonvariant peritectic equilibrium P_3 (III – 66––100 mol % Sn), with some differences in concentration ranges. As a result, dep-

ending on the concentration, a mixture of Bi+Bi_3Ni+Ni_3Sn_2, Bi+Bi_3Ni_2+Sn or Ni_3Sn_2+Ni_3Sn_4+Sn phases precipitates in the subsolidus.

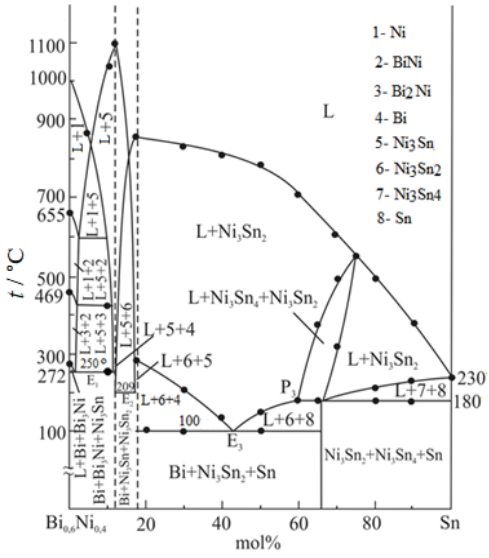

Fig. 3. Phase diagram of the $Bi_{0.6}Ni_{0.4}$–Sn section.

$Bi_{0.57}Sn_{0.43}$–Ni Section

This section is perpendicular to the non-quasibinary sections we have described (Fig. 4). $Bi_{0.57}Sn_{0.43}$ is the only binary eutectic (e_7) composition observed in the Bi–Sn system. Studying the phase equilibrium in the $Bi_{0.57}Sn_{0.43}$–Ni section allows us to follow the chemical interaction occurring in the following subsystems of the Bi–Ni–Sn ternary system: Bi–Ni–Ni_3Sn_4 (I), Bi–Ni_3Sn–Ni_3Sn_2 (II) and Bi––Ni_3Sn_2–Sn (III). The phase diagram is non-quasibinary, and the nature of the chemical interaction there is complex.

The $Bi_{0.57}Sn_{0.43}$–Ni section passes through four primary crystallization fields and intersects three monovariant curves. Therefore, the liquidus of the phase diagram consists of four branches of primary crystallization (Sn, Ni_3Sn_2, Ni_3Sn and Ni).

In the concentration range of 0–44 mol % Ni, the investigated section passes through the region of the Bi–Ni_3Sn_2–Sn (III) subsystem, and crystallization ends at 100 °C in the four-phase ternary eutectic equilibrium (L ↔ Bi + Ni_3Sn_2 + Sn). In the subsolidus, a mixture of three phases (Bi+Ni_3Sn_2+Sn) crystallizes.

In the phase diagram of the $Bi_{0.57}Sn_{0.43}$–Ni section, the chemical interaction in the Bi–Ni_3Sn–Ni_3Sn_2 (II) and Bi–Ni–Ni_3Sn (I) subsystems is further confirmed, as reflected in the previous sections. Specifically, in system (II) (44–56 mol % Ni concentration range), crystallization ends at 200 °C in the three-phase nonvariant

eutectic equilibrium (E_2, L ↔ Bi + Ni_3Sn + Ni_3Sn_2), and in the subsolidus, three phases (Bi+Ni_3Sn+Ni_3Sn_2) crystallize.

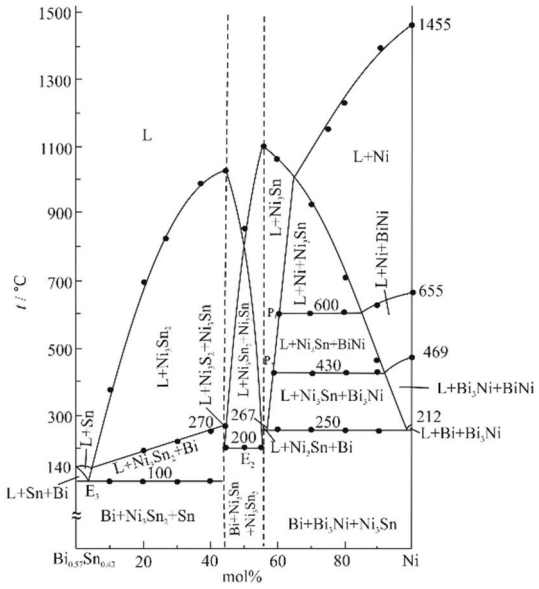

Fig. 4. Phase diagram of the $Bi_{0.57}Sn_{0.43}$–Ni section.

In the concentration range of 56–100 mol % Ni, in the region reflecting the Bi–Ni–Ni_3Sn (I) system, crystallization, as shown in the $Bi_{0.6}Ni_{0.4}$–Sn section, proceeds through the nonvariant peritectic equilibria P_1 (L + Ni ↔ BiNi + Ni_3Sn, 600 °C) and P_2 (L + BiNi ↔ Bi_3Ni + Ni_3Sn, 430 °C) and ends at the four-phase ternary eutectic equilibrium E_1 (L ↔ Bi + Bi_3Ni + Ni_3Sn, 250 °C). In the subsolidus, a mixture of Bi+Bi_3Ni+Ni_3Sn phases precipitates. It should be noted that, as can be seen from the phase diagrams, each of the investigated non-quasibinary sections has corresponding two-phase crystallization regions between their liquidus and solidus lines, which are clearly distinguished by concentration.

Among the studied polythermal sections, a significant solid solubility region based on the initial components was observed in only one, specifically the Ni_3Sn––Bi section. Furthermore, no new ternary or more complex compounds formed in any of the sections for which phase diagrams were constructed. This highlights a discrepancy between our findings and some results reported in the literature.[6–8] The significance of our results, which demonstrate the absence of such new complex compounds, is further emphasized by the principle outlined in reference:[15] the formation of new complex compounds at the contact interface of interacting metals, potentially due to localized heating, can lead to contact failure. Utilizing data from the literature on constituent binary systems, experimental results from the investigated polythermal sections, and analysis of additional samples not lying

on these sections, a projection of the liquidus surface for the Bi–Ni–Sn ternary system was constructed for the first time (Fig. 5).

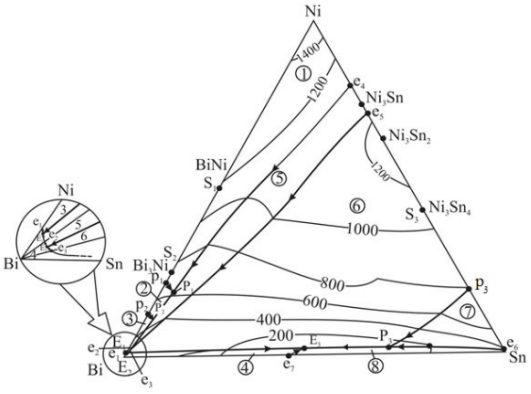

Fig. 5. Projection of the liquidus surface of the Ni–Bi–Sn ternary system with initial crystallization areas: 1 – Ni, 2 – BiNi, 3 – Bi_3Ni, 4 – Bi, 5 – Ni_3Sn, 6 – Ni_3Sn_2, 7 – Ni_3Sn_4, 8 – Sn; the phase equilibrium graph in the bismuth-rich part is highlighted in the lower left of the figure).

As can be seen from the figure, in the projection of the liquidus surface of the Ni–Bi–Sn ternary system, there are 8 primary crystallization fields characterizing the initial components and the newly formed phases, which are separated from each other by 13 monovariant curves (Table I). 7 of the 16 nonvariant equilibria existing in the projection of the system's liquidus surface are three-phase binary eutectics (e_1–e_7), 3 are three-phase binary peritectics (p_1–p_3), 3 are four-phase eutectics (E_1–E_3) and 3 are four-phase ternary peritectics (P_1–P_3).

TABLE I. Nonvariant reactions, monovariant curves, and their temperatures occurring in the Ni–Bi–Sn ternary system

No.	Nonvariant points, monovariant curves	Equilibrium reaction	t / °C
1	e_1	L ↔ Bi + Bi_3Ni	272
2	e_2	L ↔ Bi + Bi_3Sn	270
3	e_3	L ↔ Bi + Ni_3Sn_2	267
4	e_4	L ↔ Ni + Ni_3Sn	1130
5	e_5	L ↔ Ni_3Sn + Ni_3Sn_2	1160
6	e_6	L ↔ Ni_3Sn_4 + Sn	231
7	e_7	L ↔ Bi + Sn	140
8	p_1	L + Ni ↔ BiNi	654
9	p_2	L + BiNi ↔ Bi_3Ni	469
10	p_3	L + Ni_3Sn_2 ↔ Ni_3Sn_4	795
11	E_1	L ↔ Bi + Bi_3Ni + Ni_3Sn	250
12	E_2	L ↔ Bi + Ni_3Sn + Ni_3Sn_2	200
13	E_3	L ↔ Bi + Ni_3Sn_2 + Sn	100
14	P_1	L + Ni ↔ BiNi + Ni_3Sn	600
15	P_2	L + BiNi ↔ Bi_3Ni + Ni_3Sn	430
16	P_3	L + Ni_3Sn_2 ↔ Ni_3Sn_4 + Sn	180
17	e_1E_1	L ↔ Ni_3Sn + Bi	272–250
18	E_1 e_2E_1	L ↔ Bi_3Ni + Bi	250–270–200

TABLE I. Continued

No.	Nonvariant points, monovariant curves	Equilibrium reaction	t / °C
19	$E_2 e_3 E_3$	L ↔Ni_3Sn_2 + Bi	200–267–100
20	e_4P_1	L ↔ Ni + Ni_3Sn	1130–600
21	p_1P_1	L ↔ BiNi + Ni	654–600
22	P_1P_2	L ↔ BiNi + Ni_3Sn	600–430
23	P_2E_1	L ↔ Bi_3Ni + Ni_3Sn	430–250
24	e_5E_2	L ↔ Ni_3Sn + Ni_3Sn_2	1160–200
25	$E_3e_3E_2$	L ↔ Bi + Ni_3Sn_2	100–267–200
26	e_7E_3	L ↔ Bi + Sn	140–100
27	P_3E_3	L ↔ Ni_3Sn_2 + Sn	180–100
28	p_3P_3	L ↔ Ni_3Sn_4 + Ni_3Sn_2	795–180
29	e_6P_3	L ↔ Ni_3Sn_4 + Sn	231–180

The monovariant equilibrium curves were constructed based on the intersection points of the primary crystallization curves in the sections, and their directions were extrapolated according to the nonvariant equilibrium points (Table I) and the projection of the monovariant equilibrium curves drawn along the sides of the concentration triangle.

In the projection of the liquidus surface, isotherms were drawn every 200 °C by graphical interpolation. The consistency of the chemical interaction patterns observed in parallel and perpendicular polythermic non-quasibinary sections, and their mutual confirmation, leaves no doubt about the accuracy of the liquidus surface projection.

The direction of the monovariant equilibrium curves characterizing co-crystallization and the nature of the nonvariant equilibrium points (Table I) are consistent with the geometric parameters of the projection of the Ni–Bi–Sn ternary system's liquidus surface (Fig. 5).

CONCLUSION

The Ni–Bi–Sn ternary system was investigated for the first time using polythermic sections, and their respective phase diagrams were constructed. A projection of the liquidus surface for the ternary system was also determined. This projection revealed the nature of the chemical interactions, identifying 8 primary crystallization fields, 6 ternary nonvariant points and 13 monovariant curves. The absence of new ternary compound formation suggests that the synthesized alloys and eutectic compositions hold potential for use as switching and contact materials in solid-state electronics.

ИЗВОД

ПРОЈЕКЦИЈА ПОВРШИНЕ ЛИКВИДУСА ТЕРНАРНОГ СИСТЕМА Ni–Bi–Sn

CHINGIZ I. ABILOV[1] IKHTIYAR B. BAKHTIYARLY[2], SAYYARA H. SADIGOVA[1], MEHRIBAN SH. HASANOVA[1] и ELMIRA K. GASIMOVA[1]

[1]Azerbaijan Technical University, Baku, Azerbaijan u [2]Institute of Catalysis and Inorganic Chemistry named after academician M. Naghiyev of the Ministry of Science and Education of the Republic of Azerbaijan

Физичко–хемијске анализе спроведене су на шест унутрашњих политермичких пре—сека Ni–Bi–Sn тернарног система, те су конструисани фазни дијаграми тих пресека. Утврђено је да су два пресека била квазибинарна, док су четири била не-квазибинарна. Конструисана је пројекција површине ликвидуса тернарног система. Састављене су једначине за неваријантне равнотежне реакције које се дешавају у тернарном систему и одређене су њихове координате. Откривено је присуство обећавајућих подручја чврстог раствора у неким од унутрашњих пресека тернарног система, а њихове границе на собној температури су одређене. Одсуство нових комплексних једињења и присуство хомогених региона указују на то да би синтетизовани материјали могли бити погодни за примену као преклопни и контактни слојеви у алтернативним изворима енергије.

(Примљено 5. марта, ревидирано 8. маја, прихваћено 15. јуна 2025)

REFERENCES

1. M. Gurtaran, Zh. Zhang, X. Li, H. Dong, *J. Mater. Res. Technol.* **30** (2024) 7476 (https://doi.org/10.1016/j.jmrt.2024.05.136)
2. M. d'Angelo, C. Galassi, N. Lecis, *Energies* **16** (2023) 6409 (https://doi.org/10.3390/en16176409)
3. F. Garmroudi, M. Parzer, A. Riss, C. Bourgès, S. Khmelevskyi, T. Mori, E. Bauer, A. Pustogow, *Sci. Adv.* **9** (2023) (https://doi.org/10.1126/sciadv.adj1611)
4. M. Wolf, J. Flormann, T. Steinhoff, G. Gerstein, F. Nürnberger, H. J. Maier, A. Feldhoff, *Alloys* **1** (2022) 3 (https://doi.org/10.3390/alloys1010002)
5. A. Karati, V. S. Hariharan, S. Ghosh, A. Prasad, M. Nagini, K. Guruvidyathri, R. Ch. Mallik, R. Shabadi, L. Bichler, B. S. Murty, U. V. Varadaraju, *Scr. Mater.* **186** (2020) 375 (https://doi.org/10.1016/j.scriptamat.2020.04.036)
6. G. P. Vassilev, K. I. Lilova, J.-C. Gachon, *J. Alloys Compd.* **469** (2009) 264 (https://doi.org/10.1016/j.jallcom.2008.01.100)
7. S.-K. Seo, M. Cho, H. Lee, *J. Electron. Mater.* **36** (2007) 1536 (https://link.springer.com/article/10.1007/s11664-007-0256-8)
8. N. Milcheva, J. Romanowska, G. Vassilev, *Cent. Eur. J. of Chem.* **9** (2011) 149 (https://link.springer.com/article/10.2478/s11532-010-0128-6)
9. G. Vassilev, T. Kristinova, K. Lilova, J. Gachon, *J. Min. Metall., B* **43** (2007) 141 (https://doi.org/10.2298/JMMB0702141V)
10. N. Milcheva, P. Broz, J. Buršík, P. Vassilev, *Thermochim. Acta* **534** (2012) 41 (https://doi.org/10.1016/j.tca.2012.02.011)
11. Ch. Abilov, S. Sadigova, M. Hasanova, E. Kasumova, *Int. J. Mod. Phys., B* **36** (2022) 2250219 (https://doi.org/10.1142/S0217979222502198)
12. Ch. Abilov, M. Hasanova, E. Kasumova, N. Huseynova, E. Kurbanov, *AIP Conf. Proc.* **3122** (2024) 050013 (https://doi.org/10.1063/5.0216063)
13. Sh. Abdullaeva, F. Mammadov, I. Bakhtiyarly, *Zh. Neorg. Khim.* (*Russ. J. Inorg. Chem.*) **65** (2020) 98 (https://link.springer.com/article/10.1134/S0036023619110020)

14. E. N. Ismayilova, L. F. Mashadiyeva, I. B. Bakhtiyarly, M. B. Babanly, *Kondens. Sredy Mezhfaznye Granitsy* (*Condensed Matter and Interphases*) **25** (2023) 47 (https://journals.vsu.ru/kcmf/article/view/11036/11228)
15. M. I. Zargarova, K. Sh. Kakhramanov, A. A. Mageramov, R. V. Roshal, *Physicochemical basis for the selection of contact materials*, Elm, Baku, 1990 (ISBN: 5-8066-0371-7).